



The Influence of Task Objectives and Loads on the Synergies Governing Human Upper Limb Movements

Shumin Wang¹, Xiongfei Zheng¹, Ting Zhang², Jiejunyi Liang¹,
and Xiufeng Zhang³(✉)

¹ School of Mechanical Science and Engineering, Huazhong University of Science and Technology, Wuhan 430074, China

² School of Mechanical and Electric Engineering, Soochow University, Suzhou 215131, China

³ National Research Center for Rehabilitation Technical Aids, Beijing 100176, China
zhangxiufeng@nrcrta.cn

Abstract. The human upper limbs exhibit a multitude of daily functional behaviors, yet these diverse movements arise from a limited set of invariant units—synergistic bases comprising basic motion primitives. However, as human movements necessarily entails interaction with the external environment factors such as task objectives and loads may impact the synergies, thereby compromising the control of the wearable robotics based on those laws. Elucidating the influence of external factors on the synergies governing human upper limb movements presents an urgent yet unresolved challenge. The present study employed principal component analysis (PCA) to identify the distinct synergies for movements associated with differing task objectives. Comparison revealed that, for reaching movements and transferring movements, the factors exerting the greatest impact on synergies are displacement of the distal endpoints and hand grasping. For varied loads, analysis of overall similarity across synergies under different loads revealed how motion synergies changes with increased loads.

Keywords: Upper limbs · Motion synergies · Loads

1 Introduction

Motion synergies indicate that the different degrees of freedom (DoFs) among limbs are not independent of one another, and they are coupled to ensure coordinated movements of the human limbs [1]. Motion synergies are often applied in the design and control of anthropomorphic machines such as prostheses, rehabilitative exoskeletons, and assistive exoskeletons [2]. Despite the proliferation of wearable robots, human-machine interaction with these systems continues to be hampered by inadequate anthropomorphism and dexterity. In particular, undifferentiated application of the concept of common motion primitives for control exacerbates environment interaction issues for wearable

S. Wang and X. Zheng—Contributed to the work equally and should be regarded as co-first authors.

robots, especially under changing external conditions. Hence, study and elucidation of the intrinsic laws of motion manifested during human interaction with the environment, and application of these laws for control of wearable robots, may enhance rehabilitation outcomes [3] and quality of life for individuals with limb disabilities and other users.

To explore the synergies of the human upper limb movements and elucidate the mechanisms underlying their generation, researchers worldwide have conducted extensive investigations. Employing motion capture system, Bockemuehl et al. obtained spatial movement data across 10 DoFs for the arm and shoulder girdle during natural movements, extending synergy research into three dimensions. Their experiment collected single-hand capture motion data across 16 distinct trajectories [4]. By using PCA, these data revealed stable synergies of high information coverage among joints. Computational results showed that the original 10 redundant DoFs could be replaced by 3 principal components (PCs) without losing most motion information. Averta et al. proposed a dynamic means of describing human movements that incorporates time as a variable in synergies, demonstrating the temporally variant nature of synergies in human upper limb movements. Their experiment selected 30 distinct grasping target movements and recorded movement data across 7 DoFs for the right arm [5]. Extracting PCs at different points during movements and calculating temporal deviations clarified that human upper limb movement trajectories could be reconstructed through a linear combination of several major time-related functions. However, the above methods for studying motion synergies have focused solely on common motion primitives based on multi-movement averaging to maximize coverage of motion information, ignoring the impact of differences across various movement tasks and task demands.

Therefore, the presented study investigated the influence of factors such as task objectives and task demand on motion synergies. First, to obtain experimental data most representative of the impact of varied task objectives and task demands on synergies, we designed two experiments. The first experiment established a movement task with actions selected to achieve maximum coverage of upper limb motion range and hand prehension type. The second experiment, using the same actions, established a movement experiment under different loads by incrementally increasing the loads as an experimental variable. Second, to establish a dataset of multi-degree-of-freedom natural upper limb movements [6], we converted the raw data into angular displacement data across DoFs of the upper limbs. According to the relationship between points and the spatial coordinate system, we established the coordinate system and its matrix representation to obtain transformation matrices between different coordinates. Using Euler angle inverse solution, we obtained motion data under different task objectives and loads, establishing a dataset of upper limb movements. Thirdly, to explore the factors influencing multi-degree-of-freedom synergies of the upper limbs under different task objectives and their relative impacts, we conducted a comparative analysis of the synergies manifested in motion under different task objectives. Through PCA, we obtained synergies for motion data grouped by task objective [7]. Based on the variation in variance accounted for by synergies across groups and comparison of synergies, we confirmed that for reaching movements and transferring movements, the factor exerting the greatest influence was the motion path of the end effector. Finally, to clarify the influence of load on synergies, we described how synergies changed with load using load as the sole variable. Through the variance

accounted for distribution and similarity of the synergies obtained by PCA, we elucidated how motion synergies became more similar and dissimilar with increasing load, revealing the influence of load on multi-degree-of-freedom synergies of the upper limbs.

In summary, this study explored the factors influencing multi-degree-of-freedom synergies of the upper limbs during experimental actions derived from daily tasks, as well as their relative impacts. We demonstrated that the first influence was the motion path of the upper limb end effector. We investigated the influence of load on motion synergies using load as a variable. An analysis of the similarity between synergies under different loads revealed factors impacting multi-degree-of-freedom synergy movements of the upper limbs under different loads.

2 Methodology

We used coordinate transformation method and Euler angle inverse solution to obtain seven-degree-of-freedom joint angular motion data for the upper limbs and extracted synergies by PCA. By comparing synergies and groupings under different task objectives and loads, we analyzed the influencing factors and relative impacts.

2.1 Calculation of Angular Displacement Data

We converted the three-dimensional data of the observed points collected in the experiment into angular displacement to quantify upper limb joint movements. Using coordinate transformation method, we calculated the rotation angle of the coordinate system relative to the coordinate axes within each time interval. Specifically, we regarded the upper limbs as a complete kinematic chain (shoulder joint three DoFs, elbow joint two DoFs and wrist joint two DoFs), where the movements of each joint followed the principle of relative motion. By calculating the changes in the coordinates of each observed point between two adjacent time intervals, we obtained the angular displacement of each joint within those time intervals. Then, using the method of solving simultaneous equations, we calculated the absolute angular displacement of each joint within each time interval.

Assuming that three observed points are not collinear, numbered $A(x_A, y_A, z_A)$, $B(x_B, y_B, z_B)$, $C(x_C, y_C, z_C)$. The origin O is on the line formed by points A and B . Set up the coordinate system as shown in Fig. 1.

The matrix expression of the established coordinate system is

$$\begin{cases} \vec{y} = \vec{AB} \\ \vec{x}' = \vec{OC} \\ \vec{z} = \vec{x}' \times \vec{y} = \vec{OC} \times \vec{AB} \\ \vec{x} = \vec{y} \times \vec{z} = \vec{AB} \times \vec{OC} \times \vec{AB} \end{cases} \tag{1}$$

$$\mathbf{H} = [\vec{x} \ \vec{y} \ \vec{z}] \times \begin{bmatrix} \frac{1}{|\vec{x}'|} & 0 & 0 \\ 0 & \frac{1}{|\vec{y}'|} & 0 \\ 0 & 0 & \frac{1}{|\vec{z}'|} \end{bmatrix}$$

The base coordinate system in the initial state is specified as H_1 , and the moving coordinate system to be sought is specified as H_2 .

Before the motion, there is a matrix transformation between the base coordinate system and the moving coordinate system to be sought, i.e. $H_2 = H_1 \times \frac{1}{2}T$.

After the motion, the base coordinate system and the coordinate system to be sought are respectively noted as $H_{1'}$, $H_{2'}$, and the mutual relationship remains unchanged $H_{2'} = H_{1'} \times \frac{1}{2}T'$.

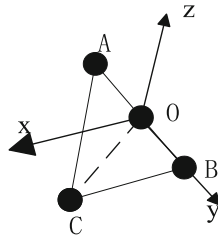


Fig. 1. Three-point spatial coordinate system.

When the motion occurs only in the base coordinate system, the transformation relationship between the coordinate system to be found and the base coordinate system does not change, i.e. $\frac{1}{2}T = \frac{1}{2}T'$.

When the coordinate system is in motion with respect to itself, there is a transformation matrix T . The transformation matrix after motion is equal to the transformation matrix when the target coordinate system does not produce motion multiplied by the transformation matrix of the target coordinate with respect to itself, that is $\frac{1}{2}T' = \frac{1}{2}T \times T$.

Combined, the rotation of the target coordinate system on itself results in

$$\begin{cases} \frac{1}{2}T = (H_1)^{-1} \times H_2 \\ \frac{1}{2}T' = (H_{1'})^{-1} \times H_{2'} \\ T = (\frac{1}{2}T)^{-1} \times \frac{1}{2}T' \end{cases} \quad (2)$$

Since the permutation matrix can be split to perform the multiplication cross of the rotation matrix around the coordinate axes, Eq. (3) is obtained in a fixed order [8].

$$T = Y_1 X_2 Z_3 = \begin{bmatrix} c_1 c_3 + s_1 s_2 s_3 & c_3 s_1 s_2 - c_1 s_3 & c_2 s_1 \\ c_2 s_3 & c_2 c_3 & -s_2 \\ c_1 s_2 s_3 - c_3 s_1 & c_1 c_3 s_2 + s_1 s_3 & c_1 c_2 \end{bmatrix} \quad (3)$$

where c_i represents the cosine of the i -th rotation angle $\cos \theta_i$, and s_i represents the sine of the i -th rotation angle $\sin \theta_i$. Subsequently, the range of angle values is determined according to the joint and the direction of the determined coordinate axis, and the data points beyond the limit position are discarded. For the purpose of description noting T as R :

$$T = R = \begin{bmatrix} r_{11} & r_{12} & r_{13} \\ r_{21} & r_{22} & r_{23} \\ r_{31} & r_{32} & r_{33} \end{bmatrix} \quad (4)$$

The inverse solution gives,

$$\begin{cases} \theta_1 = \text{Atan2}(r_{13}, r_{33}) \\ \theta_2 = \text{Atan2}(-r_{23}, r_{22}/c_3) \\ \theta_3 = \text{Atan2}(r_{21}, r_{22}) \end{cases} \tag{5}$$

Equation (3–5) always holds when the rotation angle is not equal to $\pm\pi/2$. Since the experiment data acquisition frequency was 100 Hz, the time interval between two data acquisitions was very short (0.01 s). Within this time interval, it was difficult for the upper limb joint rotation angle to reach $\pm\pi/2$, so Eq. (3–5) could be used to calculate the joint angle.

2.2 Extraction of Synergies

The goal of PCA [9] is to perform a linear combination between variables for a set of non-linearly correlated variables, and to explain the set of variables with the combined model, which generally has fewer model variables than the original variables, i.e., it achieves dimensionality reduction [10].

Define the data to be analyzed X , where there are n variables X_1, X_2, \dots, X_n , each of which is obtained by m observations, i.e.

$$X = \begin{bmatrix} X_1 & X_2 & \dots & X_n \end{bmatrix} = \begin{bmatrix} x_{11} & x_{12} & \dots & x_{1n} \\ x_{21} & x_{22} & \dots & x_{2n} \\ \vdots & \vdots & \ddots & \vdots \\ x_{m1} & x_{m2} & \dots & x_{mn} \end{bmatrix} \tag{6}$$

In this paper, we use the eigenvalue decomposition of PCA. Suppose Σ is the variance-covariance matrix of the data set, corresponding to the eigenvalue-eigenvectors $(\lambda_1, e_1), (\lambda_2, e_2), \dots, (\lambda_n, e_n)$, where $\lambda_1 \geq \lambda_2 \geq \dots \geq \lambda_n$. The i -th PC is

$$Y_i = (X - \bar{X})e_i = e_{i1}(X_1 - \bar{X}_1) + e_{i2}(X_2 - \bar{X}_2) + \dots + e_{in}(X_n - \bar{X}_n), i = 1, 2, \dots, n \tag{7}$$

The variance and covariance are respectively

$$\begin{aligned} \text{Var}(Y_i) &= e_i' \Sigma e_i = \lambda_i \\ \text{Cov}(Y_i, Y_k) &= e_i' \Sigma e_k = 0, i \neq k \end{aligned} \tag{8}$$

The first PC has the maximum variance. Each PC obtained by PCA corresponds to a variance contribution, which indicates its ability to express information in the data set. In some unserious situation, the first PC can be compared directly.

2.3 Comparison of Similarity and Clusters

By comparing the similarity and clustering grouping of synergies under different task objectives, we obtain the influence factors and relative influence degrees under different task objectives.

(1) Similarity between variables

The similarity between variables is used to show the relationship between the proximity of two groups of data, including cosine similarity, Pearson Correlation Coefficient, Jaccard coefficient, etc. Generally the larger the coefficient, the higher the similarity. Assume two variables X, Y have the sample values $(x_1, x_2, \dots, x_n), (y_1, y_2, \dots, y_n)$.

Combining the advantages, disadvantages and applicability of each similarity measure, this study uses the extended Pearson correlation coefficient [11] for cosine similarity,

$$r = \frac{\sum_{i=1}^n (x_i - \bar{x})(y_i - \bar{y})}{\sqrt{\sum_{i=1}^n (x_i - \bar{x})^2} \sqrt{\sum_{i=1}^n (y_i - \bar{y})^2}} \quad (9)$$

(2) Clustering method

There are two main approaches to cluster analysis, hierarchical clustering and non-hierarchical clustering [12]. Considering the size and content of the data in this paper, the hierarchical clustering method is mainly used. The goal of hierarchical clustering is to partition and aggregate several groups of objects to be determined into new combinations, using distance values as a metric.

The specific procedure for hierarchical clustering of objects with N objectives is:

- (a). Take N targets and form an $N \times N$ distance matrix $\mathbf{D} = \{d_{ij}\}$, where the element d_{ij} denotes the distance between the i -th target and the j -th target.
- (b). Find the two different targets U and V that are closest in distance from the distance matrix with the distance d_{UV} and grouped as (UV) .
- (c). Remove the rows and columns corresponding to UV from the matrix, add the grouping (UV) , and calculate the distance value again to get the new matrix.
- (d). Repeat steps (b) and (c) ($N-1$ times) until all targets are grouped into one grouping, and record the result of each grouping and the distance value at the time of grouping.

3 Upper Limb Motion Synergy Data Acquisition Experiment

This study employed an optical motion capture system (Vicon MX) from Vicon Metrics Limited (Oxford, UK) with a real-time sampling frequency of 100 Hz. The system consisted of multiple high-speed infrared cameras and other hardware devices. The Vicon system used Vicon Vegas sensors with proprietary patents, which offered high resolution, high capture frequency, and good three-dimensional reconstruction. The cameras collected real-time changes in the reflective markers. Using software, we obtained real-time change data for the coordinates of the reflective markers during the experiment. We determined the joint motion coordinate system using three points to determine one coordinate system and calculated joint angular displacement data using the Euler angle inverse solution. There are various ways to express motion states. In this study, we used joint angular displacements to represent the motion state. Because the range of external conditions that can influence movements is very broad, this experiment was designed from two perspectives—different daily tasks and loads—to determine influencing factors and degrees of influence for subsequent calculations.

A total of 14 Marker points were used for upper limb motion data collection, corresponding to the body parts, shoulder joint, elbow joint and wrist joint, as shown in Fig. 2.

The basic principle of the experiment was that the markers would not move and remained in a relatively stable state when only the upper limbs were active. We used three markers on the chest and back. For three motion parts, namely the shoulder, elbow, and wrist, at least one coordinate axis coincided with the actual rotation axis to facilitate calculation. The markers on the upper arm and shoulder together established the shoulder joint motion coordinate system. Considering that the skin and skeleton were not completely rigid during movements, the distance between them could not be too close to avoid insignificant performance and too far to avoid mutual influence between the elbow joint markers. Therefore, we placed the markers at the middle position of the arm length. The same rationale applied to the forearm markers.

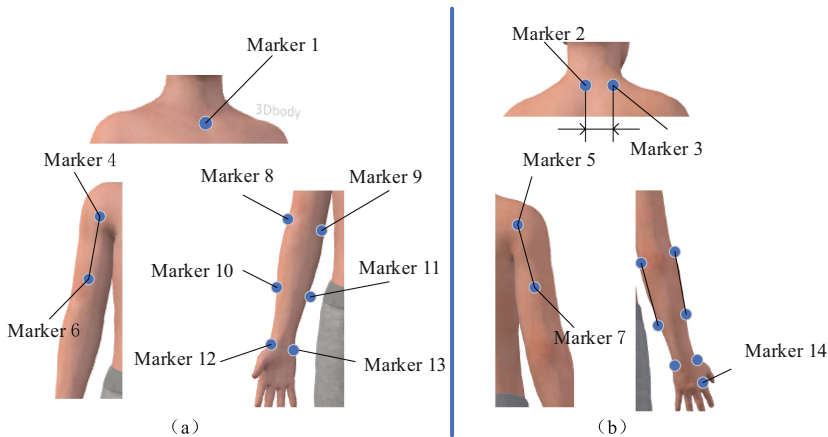


Fig. 2. Marker point location schematic. (a) The front view. (b) The back view.

3.1 Multi-task Objective Experiment

On the one hand, the muscles of arm and hand are largely shared during movement. On the other hand, most hand muscles have attachment points on the forearm. When the hand moves, both types of muscles are driven, affecting the arm movements. Therefore, hand movements directly affect arm work. According to the degree of hand involvement, the experimental actions were divided into three categories [5]: (1) reaching movements, (2) transferring movements, and (3) tool-mediated actions. Manipulation actions could not be classified or planned to meet the control variable standards and were not considered in this experiment. Reaching movements and transferring movements are a fundamental component of functional movements required for daily life. The actions selected in this experiment are highly correlated with human independent motor ability, which is helpful to extract upper limb synergies. The focus was on reaching and transferring movements. Literature [13] used the extreme position and control variable method, they obtained

the workspace that the forearm could achieve. Based on the initial sitting position, daily actions in the upper limb motion space were selected to obtain eight target actions for the first category. According to the literature [14–16], hand grasping actions were classified into 16 types based on features such as finger involvement and the size and shape of the grasped object. According to the grasping action and sitting action, seven target actions were selected for the second category. The specific classification is shown in Fig. 3.

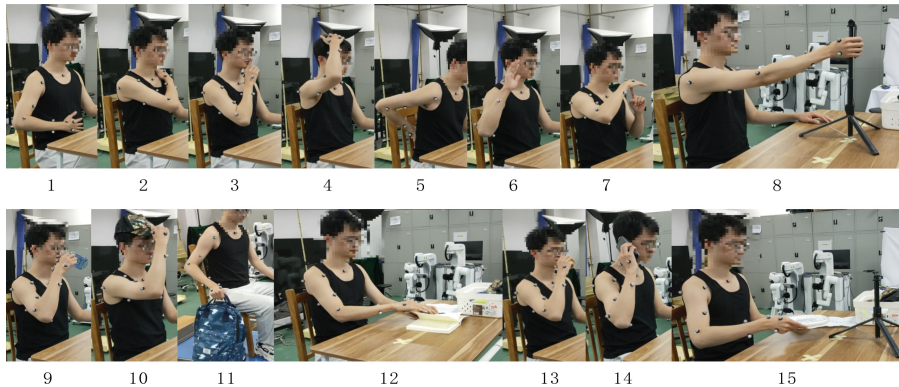


Fig. 3. Experimental action paradigm. 1 Touch the belly; 2 Touch left shoulder; 3 Make a quiet sign; 4 Touch the head; 5 Touch the back of waist; 6 Greet; 7 Make a pause sign; 8 Touch the front of chest; 9 Drink water; 10 Wear a hat; 11 Lift a bag; 12 Turn a page; 13 Eat food; 14 Ring up; 15 Put a plate.

Initial State: The sitting position was selected as the initial position with the palms facing down and naturally placed on the table. To reduce the motion errors caused by body size, the distance between the front chest and the table was the length of the subject's forearm, as shown in Fig. 4.

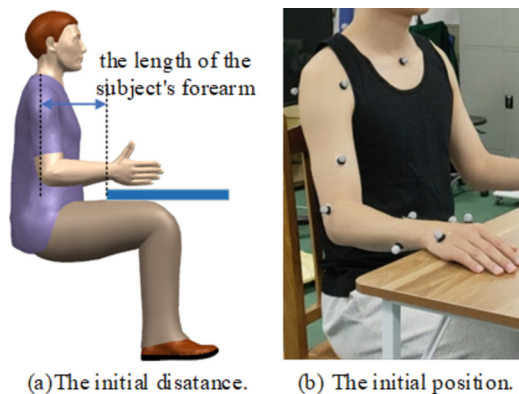


Fig. 4. Experimental Initial state. (a) The initial distance. (b) The initial position.

Experimental Process: Starting from the initial state, the subjects completed the actions sequentially according to the order shown in Fig. 4(b). After completing each target action, the initial state was restored as one set of data. 15 experimental actions were repeated 10 times for each subject as the experimental data for one person. The experiment did not strictly specify the time, but to prevent subject fatigue, there was at least a 5-s pause between each action.

Experimental Subjects: 10 healthy adults with a dominant right hand participated in this experiment. The anthropometric data of the subjects are shown in Table 1. Before the experiment, each subject was informed of the experimental content.

Table 1. Body size data of subjects in experiments with different task objectives.

Number	Height	Arm length	Forearm length	Upper arm length	Shoulder breadth
1	180 cm	62 cm	29 cm	30 cm	42 cm
2	174 cm	73 cm	26 cm	29 cm	47 cm
3	175 cm	72 cm	28 cm	33 cm	45 cm
4	187 cm	75 cm	30 cm	26 cm	47 cm
5	175 cm	73 cm	29 cm	25 cm	29 cm
6	179 cm	72 cm	29 cm	25 cm	34 cm
7	173 cm	70 cm	27 cm	24 cm	31 cm
8	178 cm	75 cm	30 cm	27 cm	30 cm
9	183 cm	75 cm	31 cm	26 cm	30 cm
10	167 cm	68 cm	25 cm	25 cm	28 cm

3.2 Experimental Setup of Upper Limb Movements Under Different Loads

Before the experiment, the Vicon system and marker positions remained unchanged.

Experimental Equipment: The experiment used 0.5 kg, 1 kg, and 2 kg dumbbells as loads. The dumbbells were placed in a briefcase as loads, as shown in Fig. 5. The empty briefcase without added dumbbells was considered No. 1. Subsequently, 0.5 kg was added each time. The maximum mass of the load equipment was 4 kg, and it was numbered 2 to 9 in sequence for record keeping.

Experimental Subjects: 10 healthy adults with right-handed dominance aged 22 to 26 years were informed of the experimental content in advance, shown in Table 2.

Experimental Process: Experimental Action 11 was selected from the experimental actions in Sects. 3.1. In order to ensure that the motion trajectory of the entire experimental movement was relatively consistent, the experimental route was required to be the same, and the initial point, end point and key way points of the entire movement process were set in advance on the reference object and remain unchanged. To reduce



Fig. 5. Load equipment.

Table 2. Body size data of subjects in experiments with different loads.

Number	Height	Arm length	Forearm length	Upper arm length	Shoulder breadth
1	180 cm	62 cm	29 cm	30 cm	42 cm
2	174 cm	73 cm	26 cm	29 cm	47 cm
3	175 cm	72 cm	28 cm	33 cm	45 cm
4	187 cm	75 cm	30 cm	26 cm	47 cm
5	176 cm	74 cm	29 cm	28 cm	46 cm
6	184 cm	75 cm	28 cm	30 cm	46 cm
7	173 cm	70 cm	27 cm	24 cm	31 cm
8	178 cm	75 cm	30 cm	27 cm	30 cm
9	182 cm	74 cm	31 cm	27 cm	30 cm
10	168 cm	69 cm	25 cm	26 cm	28 cm

errors introduced by the subject's body size, the subject's hands were naturally placed on the knees as the initial state. The initial point (or end point) of the load device was in front of the subject's feet. During the experiment, the subject needed to move the load device to the right side of their body. Placing both hands back on the knees was considered a complete experimental action. The subjects with nine different loads to completed specified experimental actions. Each load was repeated 10 times as the data for one person.

4 Analysis of the Influence Factors and the Corresponding Effects on Motion Synergies

By coordinate transformation and Euler angle inverse solution on the collected experimental data, seven-degree-of-freedom joint angle data were obtained. PCA was used to respectively extract the coordination rules of seven DoFs and five DoFs in multi-joint

upper limb motion, obtaining changes in motion synergies classified by action type. Through similarity comparison and cluster analysis of the synergies obtained, the main factors influencing the synergies were found to be the overall process of the action, the grasping situations of the hand, and the complexity of the actions in the experiment.

The load was selected as a further object of study to explore the synergies of multi-degree-of-freedom upper limb motion. Based on the synergies of the seven DoFs of upper limb motion, the synergies implied in the five DoFs of upper limb motion was explored in depth. The similarity between synergies was analyzed to reveal the influencing factors of multi-degree-of-freedom synergy motion of the upper limbs under different loads.

4.1 Analysis of Motion Synergies Under Multi-task Objectives

A total of 14 Marker points are selected in the experiment, and the data are recorded in each frame corresponds to the coordinates of the Marker points at that moment. The original data matrix \mathbf{x}_i at moment i can be expressed as:

$$\mathbf{x}_i = [x_{i,1}, x_{i,2}, x_{i,3}, \dots, x_{i,3 \times n}], n = 14 \quad (10)$$

where $[x_{i,3 \times j-2}, x_{i,3 \times j-1}, x_{i,3 \times j}]$ represents the coordinate values of the j -th Marker at moment i . Three coordinate systems are formed by 14 points (every 3–4 points form one), corresponding to shoulder joint, elbow joint and wrist joint, respectively.

A single action is repeated m times, then the data set X is represented as:

$$X = \begin{bmatrix} \mathbf{x}_1 \\ \mathbf{x}_2 \\ \vdots \\ \mathbf{x}_m \end{bmatrix} \quad (11)$$

The joint angular displacement data of the upper limbs are obtained according to the calculation in multi-task objective experiments, and the motion state is represented by the angular displacement corresponding to each moment of freedom to obtain the state matrix \mathbf{y}_i at moment i :

$$\mathbf{y}_i = [y_{i,1}, y_{i,2}, \dots, y_{i,n}], n = 7 \quad (12)$$

where $y_{i,j}$ represents the angular displacement of the j -th joint degree of freedom at the i -th moment, with m sampling points in one sampling. The state data after the k -th sampling is represented as:

$$Y_k = \begin{bmatrix} \mathbf{y}_1 \\ \mathbf{y}_2 \\ \vdots \\ \mathbf{y}_k \end{bmatrix} \quad (13)$$

Then, the state data for PCA:

$$Y = \begin{bmatrix} y_1 \\ y_2 \\ \vdots \\ y_m \end{bmatrix} \approx \begin{bmatrix} \eta_{1,1} & \eta_{1,2} & \cdots & \eta_{1,h} \\ \eta_{2,1} & \eta_{2,2} & \cdots & \eta_{2,h} \\ \vdots & \vdots & \ddots & \vdots \\ \eta_{m,1} & \eta_{m,2} & \cdots & \eta_{m,h} \end{bmatrix} \begin{bmatrix} \alpha_1 \\ \alpha_2 \\ \vdots \\ \alpha_h \end{bmatrix} + \bar{Y}, h \leq n \quad (14)$$

where the matrix $\alpha_i = [\delta_{i,1} \delta_{i,2} \cdots \delta_{i,n}]$ denotes the correspondence between the i -th PC and the joint DoFs, and η_i denotes the corresponding weights of the selected PC at moment i .

A widely view is that the upper limbs have seven DoFs. In practical applications, if seven DoFs motion synergies are used for control, the overall fault tolerance rate of the system will be low due to the characteristics of the synergies themselves (variance ratio less than 100%). If the mechanism design is directly based on the synergies of the seven DoFs of the upper limbs, there will always be deviation between the mechanical structure and the target position after the completion of the movement, and the lack of additional adjustment ability will not be able to achieve the work goal for the mechanism. Therefore, the collaborative cognition of the upper limb movement focuses on the three DoFs of the shoulder joint and the two DoFs of the elbow joint, and the wrist joint can be independently designed to consider the wrist separately and analyze the synergies of five DoFs of the upper limbs.

Considering that the seven DoFs in the upper limbs have a calibration effect, the seven DoFs were first analyzed. The variance ratios were calculated according to the numbering in the experiment, as shown in Fig. 6.

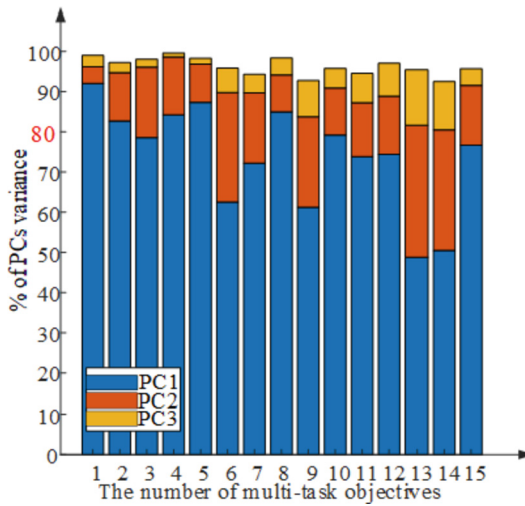


Fig. 6. Variance ratios of seven-degree-of-freedom synergies in 15 groups of movements.

A variance ratio of 80% is used as the criterion for judging whether the synergies can effectively reproduce the motion. It can be seen that the variance ratio of the first synergies fluctuate greatly, with a minimum of 45.15% and a maximum of 92.05%, indicating that the first synergies can directly replace the motion process of the corresponding group. In 15 groups of actions, the variance ratio of 5 groups is greater than 80%, indicating that at least the first synergies can be used to explain most of the motion information in these 5 groups of actions. When the first 2 synergies (the first and second synergies) are selected, the minimum variance ratio is 83.71% and the maximum is 98.57%. When the first 3 synergies are selected, the maximum variance ratio reached 99.63%, close to 100%. This means that in the seven DoFs upper limb motion, at least the first two synergies can be selected to effectively reconstruct the motion information of most actions. Judging from the range of variance ratios, the maximum difference between transferring movements and reaching movements, that is, whether the hand grasps or not, will affect the motion synergies of the upper limbs. It is speculated that the contraction of hand muscles affects the upper limb motion.

Compared with seven DoFs, five DoFs of the upper limbs omitted two DoFs: wrist flexion/extension and wrist abduction/adduction.

The motion data of five DoFs were grouped according to the actions to calculate the synergies and variance ratios, as shown in Fig. 7(a). At this time, a variance ratio exceeding 80% requires at least the first two synergies. For the first three synergies, the variance ratio of about 1/2 of the actions exceeded 99%, close to 100%. When high precision is required in applications, the first three synergies can be considered to reproduce motion. The variance ratios of the first three synergies of the five DoFs were compared with those of the seven DoFs, as shown in Fig. 7(b). In reaching movements, the variance ratios of the first three synergies are relatively close in numerical values and trends, indicating that the wrist has little effect on the synergies. In transferring movements, the trends remained close, but significant differences appeared in the numerical values in the latter half of the transferring movements. Combined with the differences between reaching movements and transferring movements, it is speculated that such differences will

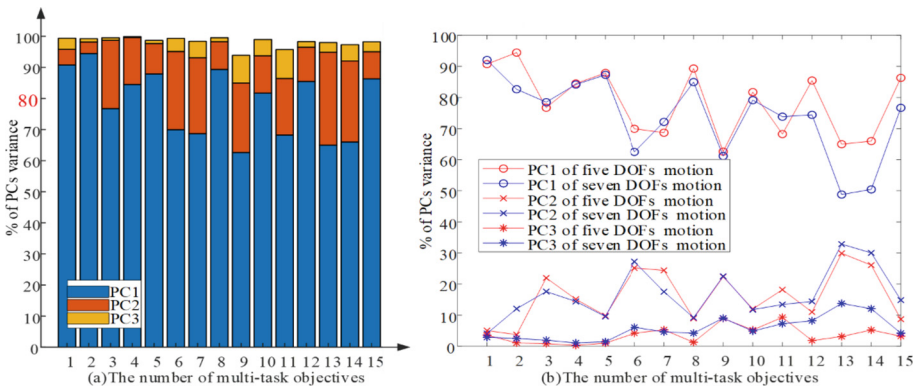


Fig. 7. (a) Variance ratios of the five-degree-of-freedom synergies in 15 sets of movements; (b) Schematic diagram of the variance ratios of the first three synergies in seven and five DoFs.

become more apparent when hand movements increase. Comparing the data of seven DoFs and five DoFs shows that wrist movements do affect motion synergies. However, according to the changes in the variance ratio of the first type of action, the influence of wrist movements is limited.

The distribution of the first synergies shows that in addition to the differences between reaching movements and transferring movements, there is another factor affecting the motion synergies. Similarity comparison and cluster analysis using the first synergies are shown in Fig. 8.

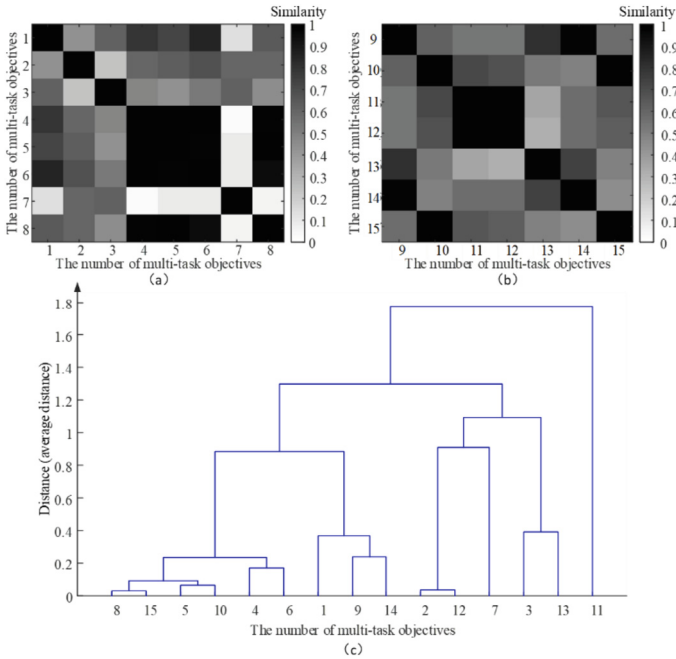


Fig. 8. (a) The similarity of first synergies in arrival action; (b) The similarity of first synergies in delivery action; (c) The clustering grouping results of first synergies.

According to the similarity in Fig. 8(a) and 8(b), it is not difficult to find that there are indeed influencing factors that cause differences in the synergies of the same type of actions, not just different variance ratios. The 15 groups of actions are grouped according to the first synergies, using the average distance as the grouping basis, shown in Fig. 8(c). According to the grouping results, the first synergies with the shortest distance do not necessarily belong to the same type of action, such as actions 8 and 15. Action 8 is a reaching movement and action 15 is a transferring movement. The common point between the two actions is that the hand passes through roughly the same position, that is, the overall action process is roughly the same. Within the experiments, the first element of the synergies is the action process without the hand. In addition, whether the hand participates in grasping and the specific requirements of the action will have a certain impact, with a relatively lower impact. However, the degree of influence of the

latter two lacks a comparison with control variables, and cannot be compared for the time being.

4.2 Analysis of Motion Synergies with Different Loads

In the load experiment, the external load mass was changed as the experimental independent variable to find the changes in motion synergies caused by changes in load mass. The synergies of seven DoFs motion of the upper limbs have not been widely used. Only preliminary cognition of seven DoFs is enough. The five DoFs motion has a wider application and needs to be calculated and analyzed from a mathematical level.

The motion of seven DoFs of the upper limbs can be effectively reconstructed using the first 2 synergies. Similarly, when the load changed, the synergies under 9 different loads were calculated in sequence. The variance ratios of the first 3 synergies under 9 different loads is shown in Fig. 9. The minimum variance ratio of the first 3 synergies is 84.25%. In addition, the first 2 synergies reach a reproduction rate of 80% in 6 conditions of 9 different loads. Therefore, the first 3 synergies are selected to represent the corresponding motion. The empty equipment weighs 1783 g. For each load group, the load increased by 500 g. Based on the first group, the second, fourth and eighth groups had the largest differences according to the total variance of the first 3 synergies. In terms of mass difference, except for the second group, the total mass of the other two groups was close to twice the total mass of the first group. It is speculated that the influence of motion synergies of two groups is related to the relative difference between different loads.

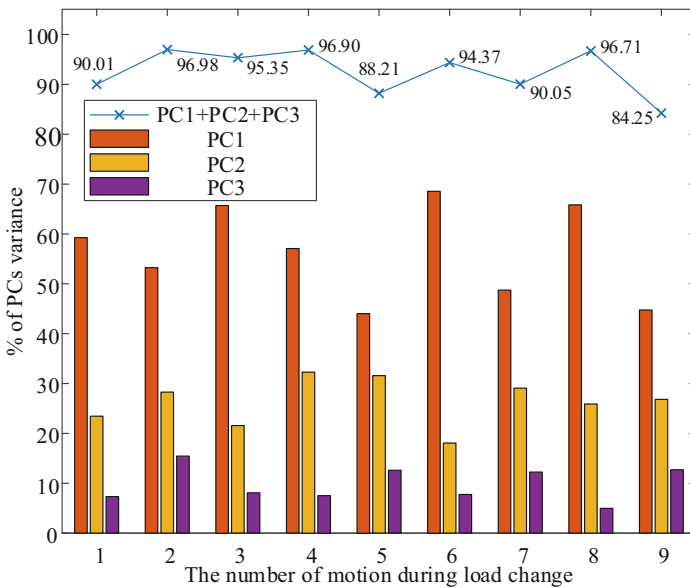


Fig. 9. Variance ratios of the first three synergies in seven DoFs.

The synergies of five DoFs of the upper limbs have a wide range of applications. An analysis of variance ratios was carried out. Groups were made according to load as the independent variable to calculate the corresponding synergies and variance ratios for each group.

The data under different task goals shows that the first 3 synergies of the five DoFs upper limb motion can reconstruct more than 90% of the information (the minimum value of group SA is 94.3197%). With 80% as the limit, only the first 2 synergies are required. According to different loads, the corresponding PCs were extracted, as shown in Fig. 10. The total variance ratio of the first 2 synergies reaches an average of 90.1122%, with a maximum of 96.1502% and a minimum of 82.8141%, exceeding 80%. This means that for occasions where high accuracy is not required, the first 2 synergies can be directly used to represent the motion under the corresponding load. For the first 3 synergies, the average variance ratio is 96.1722%, with a minimum of 91.2507%, exceeding 90%. This means that under a single load, the first 2 synergies can achieve effective reconstruction of motion, and the first 3 synergies further increase the degree of reconstruction. Further consideration will be given to the specific situation of synergies between joints under different loads.

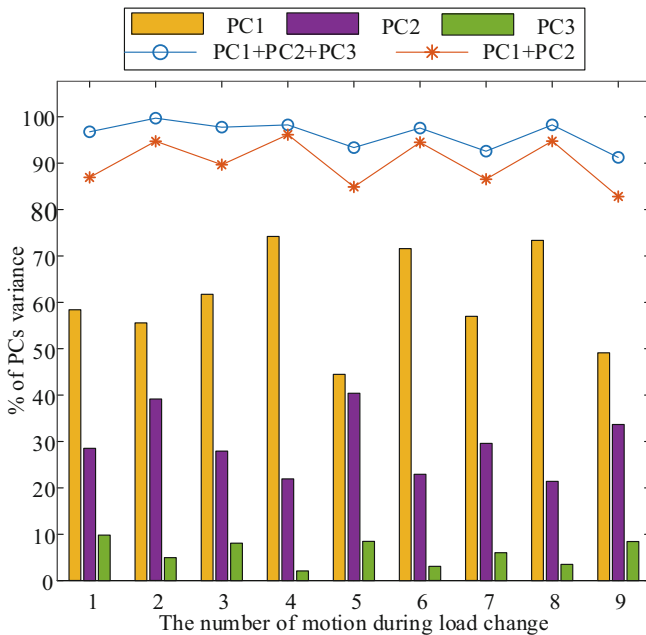


Fig. 10. Variance ratios of the first three synergies in five DoFs.

Pearson’s coefficient is used to compare the similarity of the first 3 synergies under different loads, as shown in Fig. 11(a–c). The mean similarity of the first synergies is 0.7750, the second synergies is 0.7943, and the third synergies is 0.5876. In the first and second synergies, the similarity between most groups fluctuates around 0.70, indicating that the synergies under different loads are still close. However, the low similarity in the

third synergies means that the synergies that supplements information show differences. When the load changed, the adjustment method adopted by the limbs deviated.

In the synergies of five DoFs motion, the first to fifth elements correspond to shoulder abduction/adduction, shoulder internal/external rotation, shoulder flexion/extension, elbow pronation/supination and elbow flexion/extension respectively. According to the correspondence between the coefficients in the coordinate system and the DoFs of the joints, the elements of the synergies were divided into two groups (1–3 and 4–5), forming a three-dimensional vector in the shoulder joint coordinate system and a two-dimensional vector in the elbow joint coordinate system. The length of the vector represents the degree to which the shoulder joint and elbow joint participate in the motion in the synergies. Since the synergies were standardized during calculation, the square of the vector modulus was used as a quantitative description of the proportion of the shoulder and elbow joints in the synergies, as shown in Fig. 11(d–e).

As shown in the three curves in Fig. 11, the degree of participation of the shoulder and elbow joints in the first synergies is relatively small, and the variation was small under low loads. It is believed that the first group of synergies is relatively stable when the load changed. Supplementary to the first synergies, the shoulder joint accounts for the main motion in the second synergies. Initially, the proportion of the shoulder joint is almost 1. However, the conclusions of the first and the second synergies do not apply to the third synergies. The third synergies supplements the motion reconstruction ability of

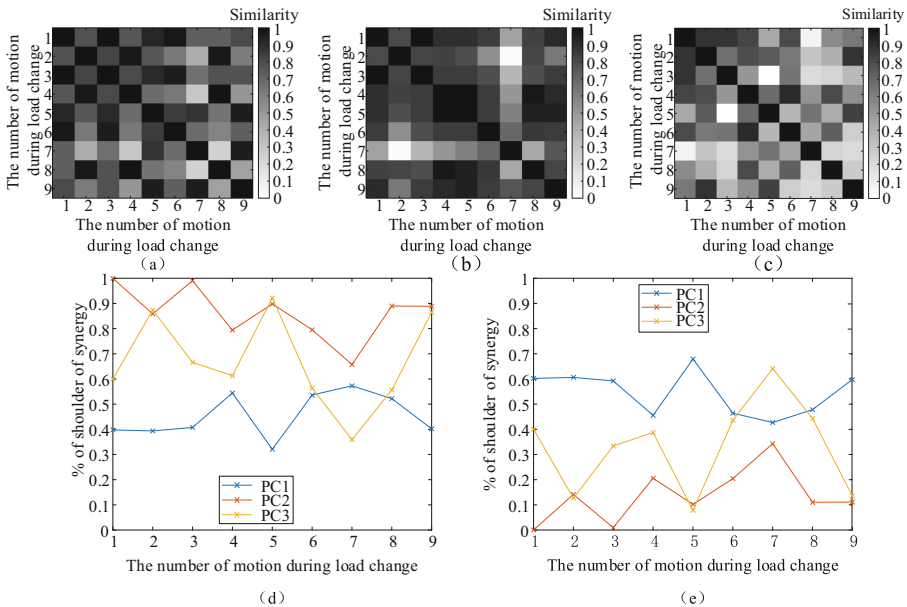


Fig. 11. (a) Similarity of the first synergies; (b) Similarity of the second synergies; (c) Similarity of the third synergies; (d) Percentage of shoulder joints in the first three synergies; (e) Percentage of elbow joints in the first three synergies. In (d) and (e), number 1 represents mass 0. Number 2 represents mass 0.5 kg. Each cell is increased by 0.5 kg. The number 9 represents maximum mass 4.0 kg.

the first two groups of synergies. It has a smaller variance ratio than the second synergies and is of less importance, belonging to secondary motion.

The muscles involved in a single motion are roughly unchanged. When the load exceeds a certain range, the physical properties (contraction rate, etc.) of the muscles differ from each other. Considering only the load factor, the properties of the muscles themselves change, and the degree of difference between the muscles also changes. As one of the factors affecting motion synergies, changes in the contraction rate of different muscles will lead to changes in synergies. In this experiment, since the loads affect all participating muscles, the final synergies changes significantly under the influence of muscles on each other.

5 Conclusion

To explore the synergies between the multi-degree-of-freedom movements of the upper limbs, starting from the daily functional activities of the human upper limbs, the upper limb movements were classified according to the workspace and hand grasp. Experimental paradigms were designed. According to the experimental data, the joint motion angles were calculated, and the synergies of the seven DoFs and five DoFs multi-joint movements of the upper limbs were extracted by PCA, respectively. Analysis of the synergies showed that the main factor affecting the synergies under multiple task goals was the movement path of the distal end of the upper limbs. To explore the synergies of upper limb movements under different loads, an upper limb movement experiment with different load masses under a single action was designed. Based on the synergies between the seven DoFs movements of the upper limbs, the synergies contained in the five DoFs movements of the upper limbs were further explored. The similarity between synergies was analyzed to reveal the influencing factors of multi-degree-of-freedom synergy movements of upper limbs under different loads. Loads change the properties of muscles and the differences between muscle group properties, thereby affecting the synergies of upper limb movements. The experimental results show that loads lead to changes in motion synergies.

Acknowledgements. This research was funded by the National Key R&D Program of China (2020YFC2007800) granted to Huazhong University of Science and Technology, and the National Natural Science Foundation of China (52005191).

References

1. Bernstein, N.A.: *The Coordination and Regulation of Movements*. Pergamon Press, New York (1967)
2. De Looze, M.P., Bosch, T., Krause, F., Stadler, K.S., O'sullivan, L.: Exoskeletons for industrial application and their potential effects on physical work load. *Ergonomics* **59**(5), 671–681 (2016)
3. Plaza, A., Hernandez, M., Puyuelo, G., Garcés, E., Garcia, E.: Lower-limb medical and rehabilitation exoskeletons: a review of the current designs. *IEEE Rev. Biomed. Eng.* **16**, 278–291 (2021)

4. Bockemühl, T., Troje, N.F., Dürr, V.: Inter-joint coupling and joint angle synergies of human catching movements. *Hum. Mov. Sci.* **29**(1), 73–93 (2010)
5. Averta, G., Valenza, G., Catrambone, V., Barontini, F., Scilingo, E.P., Bicchi, A.: On the time-invariance properties of upper limb synergies. *IEEE Trans. Neural Syst. Rehabil. Eng.* **27**(7), 1397–1406 (2019)
6. Huang, B., Xiong, C., Chen, W., Liang, J., Sun, B.Y., Gong, X.: Common kinematic synergies of various human locomotor behaviours. *R Soc Open Sci.* **8**(4), 210161 (2021)
7. Jarque-Bou, N.J., Vergara, M., Sancho-Bru, J.L., Gracia-Ibanez, V., Roda-Sales, A.: Hand kinematics characterization while performing activities of daily living through kinematics reduction. *IEEE Trans. Neural Syst. Rehabil. Eng.* **28**(7), 1556–1565 (2020)
8. Wang, K., Li, J., Shen, H.: Inverse dynamics of a 3-DOF parallel mechanism based on analytical forward kinematics. *Chin. J. Mech. Eng.* **35**(05), 307–316 (2022)
9. Hotelling, H.: Analysis of a complex of statistical variables into principal components. *Columbia Uni.* **24**(6), 417–431 (1933)
10. Dominici, N., Ivanenko, Y.P., Cappellini, G., d'Avella, A., Mondì, V., et al.: Locomotor primitives in newborn babies and their development. *Science* **334**(6058), 997–999 (2011)
11. Johnson, R.A., Wichern, D.W.: *Applied Multivariate Statistical Analysis*. Sixth Edition, pp. 524–542 (2008)
12. Johnson, S.C.: Hierarchical clustering schemes. *Psychometrika* **32**(3), 241–254 (1967)
13. Abdel-Malek, K., Yang, J., Brand, R., Tanbour, E.: Towards understanding the workspace of human limbs. *Ergonomics* **47**(13), 1386–405 (2004)
14. Santello, M., Flanders, M., Soechting, J.F.: Postural hand synergies for tool use. *J. Neurosci.* **18**(23), 10105–10115 (1998)
15. Lenarcic, J., Umek, A.: Student member: simple model of human arm reachable workspace. *IEEE Trans. Syst., Man, Cybern.* **24**(8), 1239–1246 (1994)
16. Kyota, F., Saito, S.: Fast grasp synthesis for various shaped objects. In: *Computer Graphics Forum*, vol. 31. Wiley, Hoboken (2012)